Oncology
and Radiotherapy©
18 (3) 2024: 001-009 • CASE STUDY

Targeting the warburg effect with glucose mutation theory: a two-case study on the efficacy of glucosodiene in treating metastatic triple-positive breast cancer in stage II and IV patients

Amr Ahmed[1], Maher Monir. Akl[2]

[1]The Public Health Department, Riyadh First Health Cluster, Ministry of Health, Saudi Arabia
[2]Department of Chemistry, Faculty of Science, Mansoura University, Mansoura, Egypt

ABSTRACT

This manuscript discusses the significance of Triple-Positive Breast Cancer (Estrogen Receptors Positive (ER+), Progesterone Receptors Positive (PR+), Human Epidermal Growth Factor Receptor 2 (HER2)) TPBC and the aggressive nature of Human Growth Factor Receptor 2 (HER2) in tumor development. The study focuses on the efficacy of Glucosodiene in two distinct cases: a patient with TPBC metastasized to lymph nodes in stage II, another with TPBC spread to lymph nodes, bones, axilla, breasts, peritoneum, and ovaries in stage IV; Results of the PET (Positron Emission Tomography) scan for the first case revealed positive outcomes following Glucosodiene treatment, indicating tumor disappearance and breast vitality restoration. The second case displayed metabolic response. Glucosodiene has shown promise in treating various cancer types, especially metastatic breast cancer, as demonstrated in the first case Triple-Negative Breast Cancer (TNBC) The initial case reported was of a patient suffering from metastatic triple-negative breast cancer to the bones at stage two, and her recovery was documented within 15 days of starting treatment. This case spurred further research into the use of Glucosodiene in various conditions. Promising results emerged, including the previously mentioned case and the two other cases in this study, suggesting that Glucosodiene targets different types of breast cancer receptors. The therapy targets tumor metabolic activity, based on the Glucose Mutation Theory pioneered by Maher Akl, offering a novel and effective treatment approach.

Keywords: Triple-Positive Breast Cancer (TPBC), Triple-Negative Breast Cancer (TNBC), glucosodiene therapy, maher akl theory, glucose mutation theory

Address for correspondence: Maher Monir. Akl, Department of Chemistry, Faculty of Science,Mansoura University, Mansoura, Egypt

E-mail: maherakl555@gmail.com

Word count: 5640 **Tables:** 00 **Figures:** 07 **References:** 12

Received: 26 February, 2024, Manuscript No. OAR-24-128232

Editor Assigned: 28 February, 2024, Pre-QC No. OAR-24-128232 (PQ)

Reviewed: 13 March, 2024, QC No. OAR-24-128232 (Q)

Revised: 22 March, 2024, Manuscript No. OAR-24-128232 (R)

Published: 29 March, 2024, Invoice No. J-128232

INTRODUCTION

Triple Positive Breast Cancer (TPBC), characterized by the concurrent overexpression of Estrogen Receptors Positive (ER+), Progesterone Receptors Positive (PR+), and Human Epidermal Growth Factor Receptor 2 Positive (HER2+), presents a significant clinical challenge in oncology [1]. HER2 positivity accentuates the aggressiveness of TPBC, heightening the risk of rapid disease progression and metastasis. Amplification of the HER2 proto-oncogene intensifies signal transduction pathways, fostering uncontrolled cellular proliferation [2]. Notably, TPBC often exhibits lymph node involvement, substantially increasing the likelihood of distant metastases, underscoring its intricate pathophysiology. Current therapeutic strategies predominantly revolve around targeted therapies, such as anti-HER2 agents like trastuzumab and pertuzumab, aimed at inhibiting HER2-mediated signaling pathways to impede tumor growth. Despite notable advancements, treatment challenges persist, including therapeutic limitations and the emergence of resistance [3]. The multifaceted nature of TPBC necessitates a comprehensive approach integrating chemotherapy, endocrine therapy, and HER2 targeted agents. However, the emergence of resistance mechanisms underscores the need for ongoing research into novel therapeutic avenues [4].

Maher Akl's glucose mutation theory has paved the way for the development of Glucosodiene, offering promising prospects in targeting the Warburg effect prevalent in tumors reliant on anaerobic glucose metabolism [5]. Positive outcomes have been observed, exemplified by a case study demonstrating significant improvements in a patient with metastatic triple-negative breast cancer following Glucosodiene treatment. Following the established treatment protocol demonstrated in a case of Triple-Negative Breast Cancer (TNBC) remission, and after rigorous safety evaluations within the physiological context, Glucosodiene is synthesized through a chemical reaction involving 3.5 grams of dextrose and 2.5 grams of sodium bicarbonate in a carefully filtered aqueous solution of 100 milliliters. This synthesis procedure involves controlled heating for approximately 120 seconds, calibrated to coincide with the appearance of gas bubbles, indicating the liberation of carbon dioxide. The recommended therapeutic dose of Glucosodiene is administered orally once daily, every 24 hours, in a volumetric dose of 100 milliliters. It is explained that within each 100 milliliters of the Glucosodiene solution, there is an indicative dose of Glucosodiene equivalent to

85.71 milligrams per kilogram of body weight [5, 6].

This study evaluates the efficacy of Glucosodiene in two cases: a 35-year-old woman with stage II TPBC, a 36-year-old woman with stage IV TPBC. Glucosodiene showcased effectiveness, highlighting its potential as a viable alternative in cancer treatment.

CASE PRESENTATION

Case I

The patient, a 35-year-old woman of mixed Caucasian and Arab descent, has been diagnosed with an intricate case of stage II triple-positive breast cancer. The malignancy exhibits lymph node metastasis, underscoring its advanced nature. Notably, the patient has no family history of cancer. This case signifies a complex manifestation of triple-positive breast cancer in a relatively young patient, emphasizing the advanced stage and aggressive nature of the malignancy.

Clinical indings timeline:

In the intricate case of a 35-year-old woman devoid of prior oncological history, the clinical findings unfold a compelling narrative. During her routine monthly breast self-examination, a palpable mass of significant proportions was detected in the right axillary region. This sizable lump was accompanied by an electric-like pricking sensation localized to the lymph node areas, introducing a distinctive neuropathic element to the clinical presentation. Concurrently, observable changes in breast morphology manifested, including breast sagging, constriction of the areolar halo, and atrophy at the forefront of the nipple.

On November 12, 2023, initiating a meticulous evaluation through Bilateral Digital Soft Tissue Mammography and High-Resolution Breast Sonography. The findings reveal scattered glandular condensations with an ACR density classification of B, accompanied by multiple clusters of suspicious microcalcifications. Calcified spiculated lesions in the right Upper Outer Quadrant (UOQ) were detected, measuring 13 mm x 11 mm at 9 O'clock, and an ill-defined 12 mm x 9 mm lesion at 12 O'clock. The left breast exhibits normal findings Breast Imaging Reporting and Data System 1 (BIRADS 1), while the right side indicates suspicious lesions (BIRADS 4C), warranting additional investigations through dynamic contrast (Magnetic Resonance Imaging) MRI and US-guided core needle tissue sampling with subsequent histopathology.

BIRADS classification delineates risk levels, with 0% risk for BIRADS 1 and 2, 2% for BIRADS 3, and 50% for BIRADS 4. The left breast falls into BIRADS 1, signifying a normal study, while the right side is categorized as BIRADS 4C, implying probable malignancy and necessitating further investigations. The characteristics of the lesions and lymph nodes suggest potential infiltration. Left axillary lymph nodes exhibit non-specific features (Figure 1).

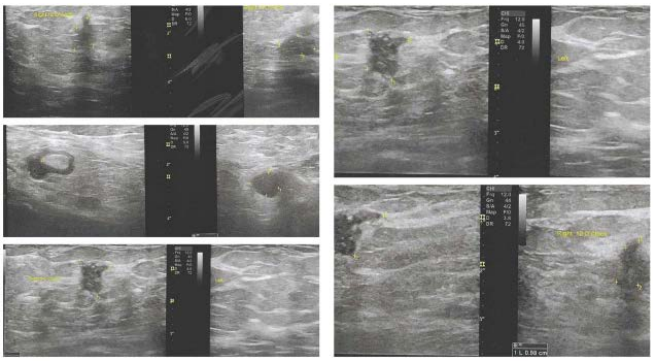

Fig. 1. In-depth assessment commenced with Bilateral Digital Soft Tissue Mammography and High-Resolution Breast Sonography, meticulously revealing diffuse glandular condensations typified by an ACR density classification of BIRADS. Concurrently, numerous clusters of suspicious microcalcifications manifested, with calcified spiculated lesions in the right Upper Outer Quadrant (UOQ) measuring 13 mm x 11 mm at 9 O'clock and an ill-defined 12 mm x 9 mm lesion at 12 O'clock. The left breast presents unremarkable findings (BIRADS 1), contrasting with the right side denoted by suspicious lesions (BIRADS 4C). The BIRADS classification system stratifies risk, associating 0% risk with BIRADS 1 and 2, 2% with BIRADS 3, and 50% with BIRADS 4. The left breast aligns with BIRADS 1, indicative of a normative study, while the right side merits a classification of BIRADS 4C, suggesting potential malignancy and necessitating additional scrutiny. Notably, the lesion characteristics, coupled with lymph node observations, intimate possible infiltration. The left axillary lymph nodes exhibit non-specific features

On November 27, 2023, a High Field Dynamic MRI of Both Breasts was conducted, employing various techniques such as axial T2 (plate 1), axial STIR (plate 2), sagittal post-contrast 3D TFE of the right breast (plate 3), sagittal post-contrast 3D TFE of the left breast (plate 4), dynamic multiphase post-contrast study done in 8 minutes with Maximum Intensity Projection (MIP) reconstruction (plate 5), and time intensity curves (plate 6).

The findings indicate bilateral glandular condensation with homogeneous glandular enhancement.

In the right breast Upper Outer Quadrant (UOQ), a partially ill-defined non-mass lesion measuring about 2 cm x 1.5 cm is observed. The lesion exhibits low signal in T2 and STIR, and the kinetic data suggests a suspicious pattern with rapid rise followed by a plateau (Type 2 curves). Two small suspicious enhancing nodules are detected in the UOQ midline, located at the 12:00 position peripheral and midzonal, measuring 8 mm x 7 mm and 12 mm x 10 mm in diameter.

These lesions also display low signal in T2 and STIR with suspicious kinetics (Type 2 plateau curves).

Associated mild diffuse skin thickening and edema are noted. Pathologically enlarged right axillary lymph nodes are observed, showing a globular appearance, with the largest measuring 2.5 cm in diameter. No masses or architectural distortion is found in the left breast, and the skin thickness and contour are normal. Multiple likely non-specific left axillary lymphadenopathy is identified. The right breast UOQ exhibits highly suspicious multifocal lesions with skin changes and ipsilateral lymphadenopathy, categorized as BIRADS 5 based on morphological and kinetic data. A microbiopsy is recommended. Conversely, the left breast study is deemed normal, categorized as BIRADS 1.

On December 9, 2023, a comprehensive evaluation encompassing microbiospy and immunohistochemical analyses was conducted, shedding light on the intricate details of the diagnostic process. Four specimens were meticulously assessed, originating from two masses situated at 12 O'clock and 9 O'clock in the right breast. Each mass provided multiple grayish-white tissue cores, measuring 0.8 cm. The ensemble included four unstained films and a syringe containing hemorrhagic material (0.2 cm x 0.2 cm). Under microscopic scrutiny, distinct characteristics emerged in the two specimens. Specimen manifested irregular groups of malignant ductal cells, displaying moderate nuclear pleomorphism, hyperchromasia, attempts at tubular formation, scattered mitotic figures, moderate desmoplasia, peritumoral lymphocytic infiltrate (5%), focal necrosis, and an intraductal component (5%) with a comedo pattern. In contrast, specimen exhibited infiltrated breast tissue with irregular groups of malignant ductal cells, moderate nuclear pleomorphism, hyperchromasia, poor attempts at tubular formation, predominantly arranged strands and cords, scattered mitotic figures, and moderate desmoplasia, devoid of necrosis or intraductal components. Cytological examination of films and cell block brought to the forefront red blood cells and hyperchromatic cells within eosinophilic proteinaceous material. The cell block revealed malignant epithelial cells with moderate nuclear anaplasia surrounded by mature lymphocytes. Immunohistochemistry analysis underscored positive staining for estrogen receptors (35% and 15% in Block 1 and Block 2, respectively), progesterone receptors (45% and 15% in Block 1 and Block 2, respectively), Her2 positivity with a score of 3+, and Ki67 proliferation indices of 30% and 20% in Block 1 and Block 2, respectively.

On December 23rd, 2023, a F-FDG Positron Emission Tomography Scan (PET/CT) examination was conducted for a female patient with a history of pathologically confirmed infiltrating duct carcinoma grade IIa in the right breast. The examination protocol encompassed a whole-body PET/CT study and a diagnostic multislice CT examination. PET/CT findings: Within the right breast, an FDG-avid enhancing nodular lesion in the LOQ exhibited an SUVmax of 14.4 with associated calcification. Additional smaller nodular lesions and soft tissue thickening in the UOQ showed an SUVmax of 3.0 over a 1.2 cm nodule, with no evidence of skin or chest wall invasion. FDG-avid lymph nodes were identified in the right axillary levels 1, II, and III, with an SUVmax of 25.3. An infraclavicular lymph node displayed an SUVmax of 15.9. Left axillary levels I and II lymph nodes exhibited an SUVmax of 7.9. Increased FDG activity was noted in the cervical right level II lymph node. Pulmonary and bone assessments revealed no FDG-avid lesions. The liver displayed mild fatty changes with a likely cyst in segment V. No FDG-avid lesions were found in the left breast. The right thyroid exhibited an FDG-avid nodule with an SUVmax of 10.6. Brain imaging revealed no FDG-avid lesions. Low-grade FDG activity was identified in subcutaneous fat stranding in the chest, abdomen, pelvis, and back, requiring clinical correlation. Similarly, low-grade FDG activity related to the endometrium and adnexae was noted, likely functional (Figure 2).

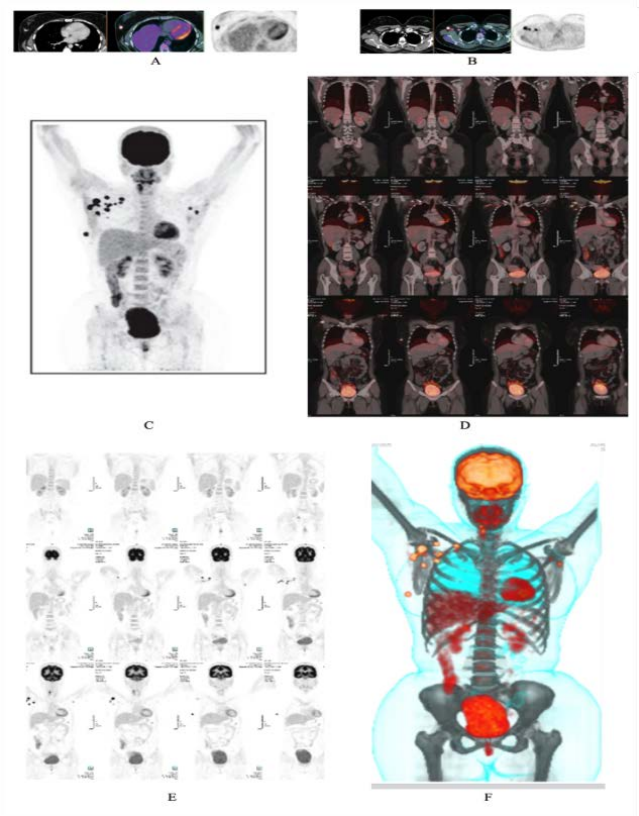

Fig. 2. Conducting a comprehensive F-FDG PET/CT examination for a female with a confirmed history of grade IIa infiltrating duct carcinoma in the right breast yielded intricate findings. Noteworthy discoveries include an FDG-avid nodular lesion in the LOQ of the right breast, exhibiting a high SUVmax of 14.4, along with associated calcification. Additionally, smaller nodular lesions and soft tissue thickening in the UOQ displayed an SUVmax of 3.0 over a 1.2 cm nodule, with no signs of skin or chest wall invasion.
The right axillary levels 1, II, and III contained FDG-avid lymph nodes with a significant SUVmax of 25.3, and an infraclavicular lymph node exhibited an SUVmax of 15.9. Conversely, left axillary levels I and II lymph nodes had a lower SUVmax of 7.9. Pulmonary and bone assessments revealed no FDG-avid lesions. The liver displayed mild fatty changes, along with a probable cyst in segment V, without FDG-avid lesions. The left breast showed no abnormal FDG uptake

On January 1, 2024, a treatment protocol was established for the patient, encompassing traditional chemotherapy administered by oncologists. The regimen consisted of alternating sessions of carboplatin and taxol at reduced doses on a weekly basis, spanning four months. Subsequently, the patient will undergo a complete mastectomy, including the breast and axillary regions.

On January 12, 2024, she opted for Glucosodiene treatment due to the lack of perceived improvements, the tumor's increasing size, and a rapid deterioration in overall health, as evident in the image before Glucosodiene treatment. During the initial preparation phase, 24 hours to 48 hours before Glucosodiene treatment, the patient strictly adhered to a specialized diet, eliminating all sources of glucose, sugars, and carbohydrates. The nutritional plan emphasized a balanced intake of animal and plant proteins, legumes, and various vegetables. Throughout the 20-day treatment period, fruits, sugars, and starchy foods were strictly avoided.

To ensure optimal digestion, a daily blend of yogurt and chia seeds was incorporated, promoting the activation of beneficial probiotics and facilitating smooth bowel movements. Chia seeds, a potent source of fiber, contributed to overall digestive well-being, and healthy fats were sourced from olive oil and assorted nuts, enhancing the nutritional composition of meals [7, 8].

The patient followed the same Glucosodiene protocol reported and documented in the initial case, involving the administration of 100 ml of Glucosodiene orally once daily for a limited duration of 20 days. Importantly, the patient continued traditional chemotherapy during the Glucosodiene treatment, receiving alternating doses of carboplatin and paclitaxel weekly to maintain a comprehensive therapeutic approach. During the Glucosodiene treatment course, the patient received only one dose of carboplatin and one of taxol, both at reduced concentrations.

Following the administration of Glucosodiene orally at a daily dose of 100 ml for 20 consecutive days, notable changes were observed in the breast and axillary regions. Starting from the fifth day, vital indicators of breast and axillary appearance began to manifest. These indicators included the restoration of the breast to its natural form before and after Glucosodiene treatment, as illustrated in the Figure 3 and Figure 4.

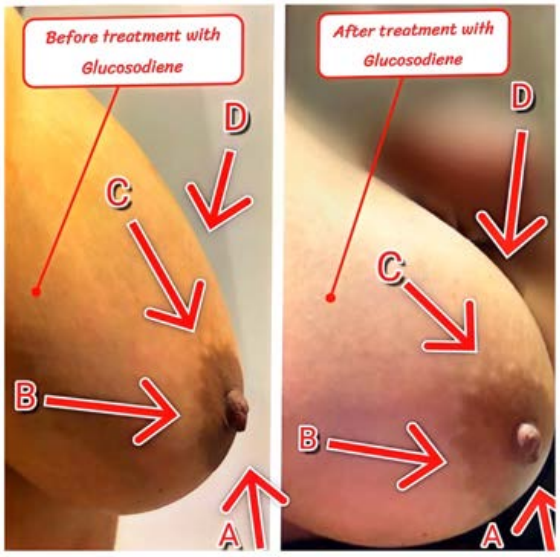

F3

Fig. 3. The figure depicts notable differences before and after treatment according to the indicated letters. Symbol (A) denotes the retraction of the nipple before treatment, contrasting with its erect appearance after the intervention. Symbol (B) signifies the constriction followed by dilation of the areolar area, while symbol (C) illustrates the atrophy of the areola specifically in the upper part of the breast before and after treatment. Conversely, symbol (D) conveys the ptosis of the breast before and after treatment. Hence, all improvements can be summarized by the fact that the breast image before commencing direct Glucosodiene treatment closely resembled the general visual indicators of breast cancer, whereas post-treatment, the breast exhibits a markedly natural and vibrant appearance

F4

Fig. 4. The figure highlights the notable differences before and after treatment for a case of metastatic triple-positive breast cancer involving lymph node metastasis at stage two, as classified by pathological reports and PET scan imaging. The tumor and lymph node swelling were visibly prominent, and the tumor size could be discerned by the naked eye throughout the treatment phases. The initial reduction in tumor growth began on the fifth day and continued until complete tumor regression by the twentieth day, indicative of tumor lysis syndrome, demonstrating the effectiveness of Glucosodiene

Upon the disappearance of the tumor and the restoration of breast vitality, a subsequent PET scan was conducted on February 3, 2024. The results indicated the following: No metabolically active cervical or supra-clavicular lymph nodes were noted in the head and neck region. The brain exhibited normal FDG bio-distribution with physiologic FDG uptake in the oropharynx, salivary glands, and larynx. An FDG-avid hypodense nodule in the right thyroid lobe was identified. In the chest, minimal diffuse skin thickening in the right breast was observed, along with scattered insignificantly avid ill-defined glandular tissue.

No metabolically active lesions were found in the left breast. Bilateral non-FDG-avid axillary lymph nodes were noted.

Moving to the abdomen and pelvis, no evidence of hepatic or splenic FDG-avid focal lesions was found. No metabolically active pelvi-abdominal lymph nodes or FDG-avid adrenal or peritoneal nodules were observed. Lastly, in the musculoskeletal system, no metabolically active sclerotic or lytic osseous deposits were found, and focal FDG avidity within the muscles of the left forearm, likely due to strain, was noted. In conclusion, the PET/CT study demonstrated positive outcomes, showcasing the effectiveness of Glucosodiene in inducing favorable changes in the breast and axillary regions, along with the absence of metabolically active lesions in various anatomical sites. The restoration of breast vitality and the absence of active lesions in follow-up imaging suggest a positive response to the treatment protocol (Figure 5).

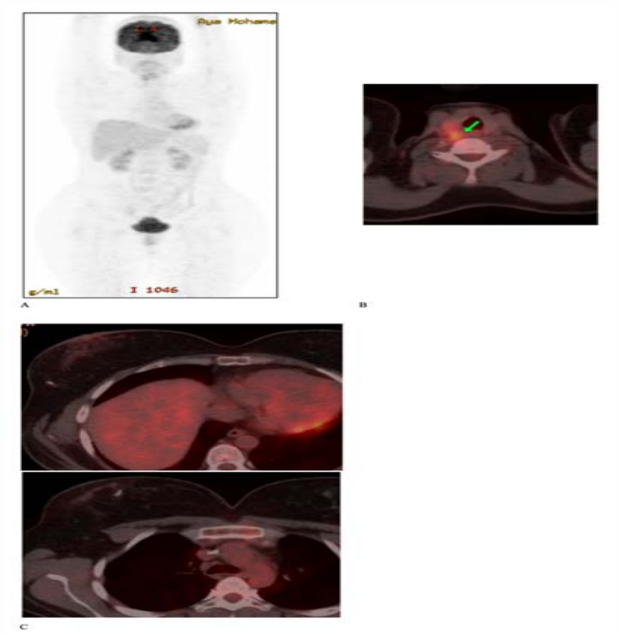

Fig. 5. Following tumor disappearance and breast vitality restoration, a subsequent PET scan indicated positive outcomes. Notably, no metabolically active cervical or supra-clavicular lymph nodes were detected, and the brain exhibited normal FDG bio-distribution. An FDG-avid hypodense nodule was identified in the right thyroid lobe. In the chest, minimal diffuse skin thickening in the right breast and insignificantly avid ill-defined glandular tissue were observed. No metabolically active lesions were found in the left breast, and axillary lymph nodes were non-FDG avid bilaterally.
Moving to the abdomen and pelvis, no hepatic or splenic FDG avid focal lesions were were found. There was an absence of metabolically active pelvi-abdominal lymph nodes, as well as FDG avid adrenal or peritoneal nodules. In the musculoskeletal system, no metabolically active sclerotic or lytic osseous deposits were present. Focal FDG avidity within the muscles of the left forearm, likely due to strain, was noted. The PET/CT study demonstrated the effectiveness of Glucosodiene, with the absence of active lesions in follow-up imaging suggesting a positive response to the treatment protocol

The presented immunohistochemistry reports detail the diagnostic findings of a patient's breast tumor before and after treatment with Glucosodiene. Before treatment, two biopsy blocks were analyzed, designated as Block 1 and Block 2, revealing notable differences in receptor expression and proliferation indices. Block 1 exhibited strong positivity for Estrogen and Progesterone Receptors (ER and PR), along with HER2 overexpression and a Ki67 proliferation index of 30%. In contrast, Block 2 demonstrated lower positivity for ER and PR, with a reduced Ki67 index. Following a 20-day regimen of Glucosodiene treatment, a subsequent biopsy report revealed changes in receptor status and proliferation indices. Before treatment, Block 1 displayed a high positivity rate for ER (35%) and PR (45%), indicative of hormone receptor positivity, while Block 2 exhibited slightly lower receptor positivity. Notably, both blocks exhibited HER2 overexpression, scored as 3+, indicating aggressive tumor behavior. Additionally, the Ki67 index, a marker of proliferation, was higher in Block 1 compared to Block 2. Post-treatment, the immunohistochemistry report indicated a significant change in receptor expression and proliferation indices. The ER and PR statuses shifted to negative in both blocks, signifying a loss of hormone receptor positivity following Glucosodiene treatment. However, HER2 overexpression persisted, suggesting resistance to the therapeutic intervention. The Ki67 proliferation index remained elevated, albeit slightly reduced compared to the pre-treatment values.

Case II

This case pertains to a, 36-year-old lady patient of Caucasian and Arab descent, with a notable family medical history, including pancreatic cancer in an aunt, stomach cancer in an uncle, uterine cancer in another aunt, and colon cancer in her grandfather.

Clinical findings timeline:

The patient has been under medical surveillance since March 2021 for left-sided breast carcinoma, characterized by positivity for Estrogen Receptors Positive, Progesterone Receptors Positive, and Human Epidermal Growth Factor Receptor 2 Positive, (ER+, PR+, HER2+), The tumor exhibited a high proliferation index (Ki-67 at 50%) and demonstrated axillary lymph node involvement. Additionally, an lytic lesion at the T11 vertebra was noted upon diagnosis [9].

Treatment initiation involved a regimen comprising paclitaxel/perjeta/herceptin, administered for 5 cycles, followed by maintenance therapy with perjeta/herceptin [10, 11]. In January 2022, due to osseous progression, the regimen was switched to kadcyla, with the patient receiving 15 cycles until October 2022. Subsequently, ENHERTU was commenced. However, treatment was prematurely halted after the 4th cycle of enhertu due to the patient's travel plans [12].

Upon her return, the patient presented with severe cervical pain and paresthesia in the left upper limb in September. A PET-CT scan conducted on September 8, 2023 revealed progression of disease involving the breast, lymph nodes, and bones (Figure 6).

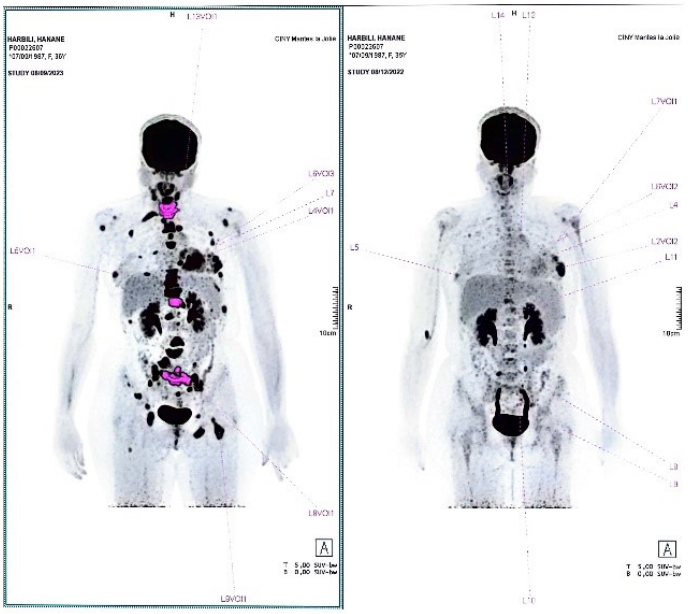

Fig. 6. On September 8, 2023 In the cervico-encephalic region, no suspicious hypermetabolic focus was observed in the cerebral area, nor in the cervical lymph nodes or upper aerodigestive tract. Similarly, no abnormal hypermetabolic focus was detected in the thoracic pulmonary area. Regarding the evaluation of the breast mass, morpho-metabolic stability was noted in the left breast mass at the junction of the outer quadrants, while metabolic progression was observed in the mass of the upper outer quadrant of the left breast, contiguous to the previously described lesion. Additionally, metabolic progression was detected in the focus at the junction of the upper quadrants of the left breast. Morpho-metabolic progression was also noted in the previously described focus at the junction of the outer quadrants of the right breast. In the axillary lymph nodes, there was morpho-metabolic progression in the previously described left axillary lymph nodes, with additional involvement adjacent to the outer border of the pectoralis minor muscle. Moving to the abdomino-pelvic region, no suspicious hypermetabolic focus was identified in the liver, spleen, adrenal glands, or pancreas, nor in the para-aortic or pelvic lymph nodes. Stable increased uptake was observed in the left ovarian region, non-specific for age.

In the musculoskeletal system, marked progression was noted in the number, extent, and intensity of known secondary osseous lesions, now manifesting as lytic lesions. Notable targets included lytic lesions at various locations, with significant progression observed in the sacral lesion and the emergence of multiple intensely hypermetabolic lytic lesions. compared to the previous PET scan On December 8, 2022, there was evidence of progression in the breast lesions, axillary lymph nodes, and osseous lesions, highlighting the aggressive nature of the disease and the need for further investigation and management. An urgent MRI performed on September 15, 2023 confirmed multiple secondary spinal lesions extending from the cervical to sacral spine, complicated by pathological fractures, notably at C4, C6, C7, T1, T4, T11, T12, L4, and S1 levels. Neurosurgical consultation was sought from Hospital Foch, with additional imaging requested before therapeutic decision-making. Immediate immobilization with cervical collar and brace was implemented, alongside urgent radiotherapy

During the initial preparation phase, 24 hours to 48 hours before Glucosodiene treatment, the patient strictly adhered to a specialized diet, eliminating all sources of glucose, sugars, and carbohydrates. On 7th February 2024, the patient commenced treatment with Glucosodiene at a dosage of 100 milliliters orally daily, starting on the fifth day. Notable improvement was reported by the patient, particularly in bone pain intensity, along with regained mobility and functionality without experiencing fatigue. The patient completed a total of 15 doses of Glucosodiene, administered orally every 24 hours.

Subsequently, on February 22, 2024, a PET scan was conducted to assess treatment response (Figure 7).

Fig. 7. The PET scan conducted on February 22, 2023, showed promising results for the patient. No abnormal metabolic activity was detected in the cervico-encephalic or thoracic regions. Partial regression was noted in left breast lesions, with a positive response in axillary lymph nodes. No abnormal metabolic activity was found in the abdomino-pelvic region, with improvement seen in the musculoskeletal system. Overall, compared to the previous scan, there was a partial metabolic response to treatment, indicating positive progress in the patient's condition

In the cervico-encephalic region, no suspicious hypermetabolic focus was observed in the cervical or cerebral regions. Similarly, no abnormal hypermetabolic focus was detected in the pulmonary parenchyma. Regarding breast lesions, a partial morpho-metabolic regression was noted in the left multifocal breast lesions, while a partial morpho-metabolic response was observed in the right breast lesion. Additionally, a near-complete to complete metabolic response was observed in the left axillary lymph nodes. In the abdomino-pelvic region, no suspicious hypermetabolic focus was identified in the hepatic, adrenal, splenic, or pancreatic regions, nor in the coeliac-mesenteric, para-aortic, or pelvic lymph nodes. A partial metabolic response was observed in the left ovarian region, with no evidence of peritoneal effusion or peritoneal nodules.

In the musculoskeletal system, there was a marked regression in the number, size, and intensity of hypermetabolic osseous lesions, presenting as secondary lesions with a denser appearance. Various bones showed improvement, including the iliac wings, sacrum, pelvic branches, coccyx, ribs, sternum, clavicles, femurs, and humeri, comparative to the PET scan conducted on September 8th, 2023, there was evidence of a partial metabolic response, with improvements observed in breast lesions, axillary lymph nodes, and disseminated secondary osseous lesions. No new suspicious foci were detected. In the clinical assessment of This patient with metastatic TPBC , monitoring biomarkers such as Alkaline Phosphatase (ALP), Carcino-Embryonic Antigen (CEA), and Antigen CA 15-3 plays a pivotal role in gauging disease progression and response to treatment. Prior to initiating Glucosodiene therapy, the ALP level was markedly elevated at 700 units/L, well above the normal range of 40 units/L to 150 units/L. ALP is an enzyme predominantly found in bones and the liver, and its elevation in cases of metastatic cancer typically signifies bone involvement or liver metastasis. The significant decrease in ALP levels post-treatment to 280 units/L indicates a favorable response to Glucosodiene therapy, suggesting a reduction in tumor burden and a potential halt in disease progression. Similarly, the reduction in CEA levels from 70.3 ng/mL to 36.9 ng/mL following treatment reflects a positive response to therapy. CEA, a glycoprotein produced during fetal development, is often elevated in the presence of certain cancers, including colorectal, lung, and breast cancers. A decrease in CEA levels post-treatment suggests a regression of tumor activity and a favorable therapeutic outcome.

Furthermore, the decline in Antigen CA 15-3 levels from 146.6 KU/L to 78.1 KU/L post-treatment signifies a positive treatment response. Antigen CA 15-3 is a tumor marker primarily associated with breast cancer, and its elevation is indicative of disease progression or recurrence. The observed reduction in Antigen CA 15-3 levels following Glucosodiene therapy suggests a favorable treatment response and potential suppression of tumor activity. The rapid decline in these biomarkers within a short duration of 15 days post-initiation of Glucosodiene therapy underscores the efficacy of the treatment regimen in controlling cancer progression.

RESULTS

Case I

The patient, a 35-year-old woman of mixed Caucasian and Arab descent, presented with a complex case of stage II triple-positive breast cancer, characterized by lymph node metastasis, indicative of an advanced disease state. Following the administration of Glucosodiene orally at a daily dose of 100 ml for 20 consecutive days, notable changes were observed in the breast and axillary regions. Starting from the fifth day, vital indicators of breast and axillary appearance began to manifest, culminating in the restoration of breast vitality and the disappearance of the tumor. Subsequent imaging via PET scan revealed positive outcomes, with the absence of metabolically active lesions in various anatomical sites. Notably, the restoration of breast vitality and the absence of active lesions in follow-up imaging suggest a positive response to the treatment protocol.

Case II

The PET scan conducted on the patient, a 36-year-old woman,

following the administration of Glucosodiene orally at a daily dose of 100 ml for 15 consecutive days showed promising results, with partial regression noted in left breast lesions and a positive response observed in axillary lymph nodes. Improvement was also seen in the abdomino-pelvic region and the musculoskeletal system, indicating a partial metabolic response to treatment compared to the previous scan. Notably, there was marked regression in the number, size, and intensity of hypermetabolic osseous lesions, demonstrating positive progress in the patient's condition.

DISCUSSION

In the first case, the PET scan examination unequivocally supports Glucosodiene's role as a primary therapeutic agent for metastatic Triple-Positive Breast Cancer. Glucosodiene effectively caused the complete disappearance of all active foci in the bones within the specified treatment period, demonstrating its remarkable ability to halt tumor activity. Moreover, Glucosodiene showed compatibility with modified Carboplatin and Taxol, highlighting its safety profile in conjunction with traditional chemotherapies. The alkaline nature of Glucosodiene potentially enhances the effectiveness of chemotherapy by targeting the Warburg effect and metabolic activity of tumors. These findings position Glucosodiene as a promising companion drug for targeting tumors reliant on the Warburg effect and suggest its utility as a primary or secondary treatment modality alongside conventional therapies.

Moving to the second case, the PET scan Discussion , revealed promising results following Glucosodiene treatment. Significant improvements were observed in breast lesions, axillary lymph nodes, and disseminated secondary osseous lesions, indicating a partial metabolic response to treatment. Notably, Glucosodiene showcased its potential in inducing favorable responses in metastatic breast cancer, further reinforcing its role as a valuable therapeutic option.

Overall, the cases discussed underscore the challenges of cancer treatment, the complexities surrounding chemotherapy, and the potential of Glucosodiene as a groundbreaking alternative, showcasing positive outcomes in improving patient conditions.

CONCLUSION

This manuscript sheds light on the complexities of triple-positive and through the exploration of Glucosodiene therapy, guided by the innovative Maher Akl Theory and the Glucose Mutation Theory, we have witnessed promising results in challenging cases. The efficacy of Glucosodiene extends hope for a novel approach in cancer treatment, as demonstrated in the case reports of patients with diverse cancer subtypes. These findings underscore the importance of exploring alternative therapeutic avenues and highlight the potential of Glucosodiene as a viable option in the fight against cancer. Further research and clinical trials are warranted to elucidate its full therapeutic potential and optimize its application in clinical practice.

ACKNOWLEDGMENT

I would like to express my deep appreciation to all the dedicated researchers and healthcare professionals in the field of oncology who have devoted their time and efforts to finding effective treatments and alleviating the suffering of patients. It is my genuine aspiration that the findings of Maher Akl's theory on glucose mutation contribute, in some way, to the ultimate eradication of cancer. This noble cause is one that deserves a lifetime of dedication and collective efforts.

DECLARATION

Informed consent

Before taking this case, information was given to the patient and informed consent was obtained from the patient for follow-up and consent to share the investigations and figures and any required data.

Funding information

The authors received no financial support for the research and publication of this article.

Competing interest declaration

The authors declare that there are no conflicts of interest.

Ethical approval statement or statement of informed consent for case studies

This case was conducted in accordance with the declaration of Helsinki and meets the CARE guidelines criteria informed consent was obtained from the patient for follow up including permission for publication of all photographs, lab, and images herein. Trial registration details: NCT05957939.

REFERENCES

1. Zeng J, Edelweiss M, Ross DS, Xu B, Moo TA, et al. Triple-Positive breast carcinoma: histopathologic features and response to neoadjuvant chemotherapy. Arch Pathol Lab Med. 2021;145:728-735.
2. Freudenberg JA, Wang Q, Katsumata M, Drebin J, Nagatomo I, et al. The role of HER2 in early breast cancer metastasis and the origins of resistance to HER2-targeted therapies. Exp Mol Pathol. 2009;87:1-1.
3. Sapna FN, Athwal PS, Kumar M, Randhawa S, Kahlon S. Therapeutic strategies for human epidermal receptor-2 positive metastatic breast cancer: a literature review. Cureus. 2020;12.
4. Kinnel B, Singh SK, Oprea-Ilies G, Singh R. Targeted therapy and mechanisms of drug resistance in breast cancer. Cancers. 2023;15:1320.
5. Akl M, Ahmed A. Developing the Theory of Toxic Chemotherapeutic Nutrition for Cancer Cells and Targeting Tumors via Glucose Mutation: Medical Guidance and Integrated Therapeutic Approach. Qeios. 2024.
6. Ahmed A. Targeting the warburg effect with glucosodiene: a case report of a 43-year-old female after mastectomy of the right breast and axillary clearance with successful first case treatment for metastatic Triple Negative Breast Cancer (TNBC) of bone. Qeios. 2023.
7. Khalid W, Arshad MS, Aziz A, Rahim MA, Qaisrani TB, et al. Chia seeds (Salvia hispanica L.): A therapeutic weapon in metabolic disorders. Food Sci Nutr. 2023;11:3-16.
8. Liu AG, Ford NA, Hu FB, Zelman KM, Mozaffarian D, et al. A healthy approach to dietary fats: understanding the science and taking action to reduce consumer confusion. Nutr j. 2017;16:1-5.
9. Davey MG, Hynes SO, Kerin MJ, Miller N, Lowery AJ. Ki-67 as a prognostic biomarker in invasive breast cancer. Cancers. 2021;13:4455.
10. Smyth LM, Iyengar NM, Chen MF, Popper SM, Patil S, et al. Weekly paclitaxel with trastuzumab and pertuzumab in patients with HER2-overexpressing metastatic breast cancer: overall survival and updated progression-free survival results from a phase II study. Breast Cancer Res Treat. 2016;158:91-97.
11. McCarthy G, Bernstein A. Combating EPA rollbacks—health care's response to a retreat on climate. N Engl J Med. 2019;381:696-698.
12. Trastuzumab Deruxtecan (Enhertu) CADTH Reimbursement Recommendation Indication. Int J Geogr Inf Sci. 2023.